Clinical Immunology 268 (2024) 110357

Contents lists available at ScienceDirect

Clinical Immunology

journal homepage: www.elsevier.com/locate/yclim

Enhanced fatty acid oxidation by selective activation of PPARα alleviates autoimmunity through metabolic transformation in T-cells

Satoshi Masuyama [a], Masayuki Mizui [a,*], Masashi Morita [a,e], Takatomo Shigeki [a], Hisakazu Kato [b], Takeshi Yamamoto [a], Yusuke Sakaguchi [a], Kazunori Inoue [a], Tomoko Namba-Hamano [a], Isao Matsui [a], Tatsusada Okuno [c], Ryohei Yamamoto [d], Seiji Takashima [b], Yoshitaka Isaka [a]

[a] Department of Nephrology, Osaka University Graduate School of Medicine, Suita, Osaka, Japan
[b] Department of Medical Biochemistry, Osaka University Graduate School of Medicine, Suita, Osaka, Japan
[c] Department of Neurology, Osaka University Graduate School of Medicine, Suita, Osaka, Japan
[d] Department of Health Promotion Medicine, Osaka University Graduate School of Medicine, Suita, Osaka, Japan
[e] Department of Nephrology, NHO Osaka Minami Medical Center, Japan

ARTICLE INFO

Keywords:
PPARα
FAO
Th17
Glutaminolysis
Autoimmunity

ABSTRACT

While fatty acid oxidation (FAO) in mitochondria is a primary energy source for quiescent lymphocytes, the impact of promoting FAO in activated lymphocytes undergoing metabolic reprogramming remains unclear. Here, we demonstrate that pemafibrate, a selective PPARα modulator used clinically for the treatment of hypertriglyceridemia, transforms metabolic system of T-cells and alleviates several autoimmune diseases. Pemafibrate suppresses Th17 cells but not Th1 cells, through the inhibition of glutaminolysis and glycolysis initiated by enhanced FAO. In contrast, a conventional PPARα agonist fenofibrate significantly inhibits cell growth by restraining overall metabolisms even at a dose insufficient to induce fatty acid oxidation. Clinically, patients receiving pemafibrate showed a significant decrease of Th17/Treg ratio in peripheral blood. Our results suggest that augmented FAO by pemafibrate-mediated selective activation of PPARα restrains metabolic programs of Th17 cells and could be a viable option for the treatment of autoimmune diseases.

1. Introduction

To execute efficient immune responses, immune cells alter metabolic pathways in response to activation signals according to their energy demands [1]. The metabolism of lymphocytes undergoes dynamic regulation during their differentiation processes. Naïve, regulatory and memory T-cells in a quiescent state generate energy through fatty acid oxidation (FAO) and oxidative phosphorylation (OXPHOS) in mitochondria, enabling their long-term survival. Upon activation of naïve T-cells, increased uptake of glucose and amino acid occurs, leading to metabolic reprogramming characterized by a shift from FAO to glycolysis, amino acid metabolism, and fatty acid synthesis (FAS), facilitating effective adenosine triphosphate (ATP) production for cell proliferation and cytokine production [2–4]. While up-regulation of glucose transporters and glycolysis is essential for effector T-cell proliferation and differentiation, regulatory T-cells (Tregs) do not rely on glycolysis, or rather, excessive glycolysis could reduce Treg cell stability. In IL-17-producing T-helper (Th17) cells, which exhibit high plasticity with Tregs, the importance of glutamine metabolism as well as glycolysis has been demonstrated [5–8]. In Treg, enhancement of FAO and oxidative phosphorylation (OXPHOS) via AMPK activation was reported to promote Treg differentiation [9,10]. However, the impacts of enhancing FAO in effector T-cells are still unclear.

PPARs (Peroxisome proliferator-activated receptors) are nuclear receptors of long-chain fatty acids and lipid mediators which function as transcriptional regulators of fatty acid metabolism. The expression of PPAR subsets varies among immune cells [11]. While PPARγ is significantly expressed in antigen-presenting cells such as macrophages, PPARα is dominantly expressed in lymphocytes [12]. Although the mechanism of action from an immunometabolic perspective remains unclear, conventional PPARα agonists, gemfibrozil and fenofibrate, have been shown to alleviate clinical symptoms of experimental autoimmune

* Corresponding author.
E-mail address: mmizui@kid.med.osaka-u.ac.jp (M. Mizui).

https://doi.org/10.1016/j.clim.2024.110357
Received 10 June 2024; Received in revised form 29 August 2024; Accepted 2 September 2024
Available online 5 September 2024

encephalomyelitis (EAE) model in mice [13]. There seems to exist sex differences in the effects of PPARα agonists, with a later study suggesting that the therapeutic effects were exerted only in male mice due to the higher PPARα expression in male than in female [14].

Pemafibrate (Parmodia®, PEM), a selective PPARα modulator (SPPARMα) recently launched as an anti-hypertriglyceridemia drug in East Asia, has over 2500 times higher PPARα selectivity than conventional fibrates [15]. In the recent global, double-blind, randomized trial investigating the additional administration of PEM under strong statin therapy (PROMINENT), PEM did not reduce the risk of cardiovascular events but had a significantly lower incidence of adverse events compared with fenofibrate [16,17].

Here we show that activation of PPARα by PEM administration modifies the metabolism of effector T-cells via augmented FAO, thereby alleviating Th17-related autoimmune diseases regardless of gender. PEM does not affect Th1 or Th2 but exclusively alters the Th17/Treg balance through FAO-dependent inhibition of glycolysis and of glutaminolysis. The Th17/Treg balance was also reduced in patients treated with PEM, indicating sufficient efficacy at therapeutic doses.

2. Materials and methods

2.1. Mice

Male and female C57BL/6 J mice, female BALB/c mice at 6–10 weeks of age and female NZB/W F1 mice at 20 weeks of age were purchased from Japan SLC (Shizuoka, Japan), housed in a specific pathogen-free animal facility at The Osaka University Graduate School of Medicine in accordance with the Animal Committee of Osaka University's guidelines.

2.1.1. Experimental autoimmune encephalomyelitis (EAE) model

In brief, male and female C57BL/6 J mice were injected subcutaneously at two sites with an emulsion of 100 μl complete Freund's adjuvant prepared by mixing incomplete Freund's adjuvant (BD Biosciences) and *Mycobacterium tuberculosis* (BD Biosciences) and 100 μg MOG 35–55 (Bio-Synthesis Inc.). Mice received 200 ng *bordetella pertussis* (List Biological Laboratories, Inc) intraperitoneally at day 0 and day 2 after EAE induction. The daily clinical scores were assessed in addition to body weight measurement as follows: 0, unaffected; 1, flaccid tail; 2, impaired righting reflex and/or gait; 3, partial hind limb paralysis; 4, total hind limb paralysis; and 5, total hind limb paralysis with partial forelimb paralysis. Lymphocyte aggregation in the draining lymph nodes was evaluated by flow cytometry at day 10 and histopathological analysis of spinal cords was performed at the peak of the disease.

2.1.2. Imiquimod-induced psoriasis-like skin inflammation model

BALB/c mice at 8 weeks of age received commercially available 5 % imiquimod cream (IMQ, Mochida Pharmaceutical Co.) on the shaved back and ears for 5 consecutive days. The thickness of the ears was measured using a micrometer since the first day that IMQ was administrated for seven consecutive days. Psoriasis Area Severity Index (PASI) was used to assess the inflammatory status of the mice dorsal skin at day7. It included the visual examination of the following three parameters: erythema (redness), induration (thickness) and desquamation (scale) on the back skin. Each parameter was given a score between 0 and 4 (0-none, 1-slight, 2-moderate, 3-marked, 4-very marked) leading to a cumulative score. The evaluation was done independently by two researchers and the mean of values was then calculated. Lymphocyte aggregation in the draining lymph nodes was evaluated by flow cytometry and histopathological analysis of skins and ears was performed at day 7.

2.2. Teatment procedures

Each model in mice was randomly divided into the two groups: control group; PEM-treated group (0.1 mg/kg/day, orally administration). Treatment of EAE and IMQ-induced psoriasis were started at day1, and was started at day15 for EAE after disease onset. NZBW/F1 mice was treated from 20 weeks of age. In vitro, pemafibrate (Kowa Company Ltd.), fenofibrate (Sigma-Aldrich), etomoxir (Sigma-Aldrich) and pioglitazone (Tokyo Chemical Industry Company Ltd.) were dissolved in sterile-filtered dimethyl sulfoxide (DMSO, Nacalai Tesque Inc.) and added in medium at day0.

2.3. Human PBMCs isolation

Human PBMCs were collected from chronic kidney disease (CKD) patients with reduced renal function (eGFR <60 ml/min/1.73m^2) or urinary protein (UP/Cr > 0.15 g/gCr) and who visit to our department and gave consent. All patients do not take any immunosuppressant. Patient characteristics are shown in Supplementary Table S2.

2.4. In vitro cell culture

Mouse naïve CD4$^+$T-cell isolation kit was used to purify naive CD4$^+$T-cells from splenocytes of 6–8-week-old male C57BL/6 J mice. Purified naive T-cells were stimulated with plate-bound anti-CD3 (1 μg/ml; 2C11) and anti-CD28 (1 μg/ml; 37.51) in RPMI-1640 (Nacalai Tesque Inc.) or IMDM (Nacalai Tesque Inc.) supplemented with 10 % FBS, 100 U/ml penicillin (Gibco), 100 μg/ml streptomycin (Gibco) and 50 μM 2-mercaptoethanol (Sigma-Aldrich) for Th0, in the presence of recombinant mouse (rm) IL-12 (10 ng/ml, Biolegend) and anti-IL-4 (10 μg/ml, BioXCell) for Th1, rmIL-4 (10 ng/ml, BioLegend) and anti-IFNγ (10 μg/ml, BioXCell) for Th2, rmTGF-β (3 ng/ml, BioLegend) for iTregs, rmTGF-β (3 ng/ml), rmIL-6 (20 ng/ml, BioLegend), anti-IFNγ (10 μg/ml, BioXCell) and anti-IL-4 (10 μg/ml, BioXCell) for Th17 condition, rmIL-1β (20 ng/ml, BioLegend), rmIL-6 (20 ng/ml, BioLegend), rmIL-23 (20 ng/ml, BioLegend), anti-IFNγ (10 μg/ml, BioXCell) and anti-IL-4 (10 μg/ml, BioXCell) for pathogenic Th17 condition. Bone marrow-derived macrophages (BMDMs) were prepared from 6 to 8-week-old male C57BL/6 J mice as previously described in the presence of DMEM high glucose medium (Nacalai Tesque Inc.). BMDMs were stimulated by LPS (10 ng/ml, Sigma-Aldrich) for M1 or rmIL-4 (20 ng/ml) for M2 macrophage.

2.5. ELISA

TNF-α, IL-1β and IL-10 were measured in the supernatant of cell-cultured medium or the plasma using ELISA system (BioLegend). Anti-mouse dsDNA IgG antibodies in the plasma were measured using the ELISA system (Wako Pure Chemical Industries).

2.6. Glutamine assay

The supernatant glutamine concentrations were measured using Glutamine Assay Kit-WST (Dojindo Laboratories) at day 4 under Th17 condition.

2.7. Flow cytometry

Lymph nodes, Spleens or digested spinal cords were passed through a 40-μm cell strainer (Corning). Erythrocytes were eliminated using Red Blood Cell Lysis Buffer (Sigma-Aldrich) for 5 min at room temperature. Isolated cells were stained with the following mAbs specific for: Fc-receptor (93), CD3 (145-2C11), CD4 (GK1.5), CD8 (53–6.7), CD45 (30-F11), CD11b (M1/70), CD25 (PC61), 7AAD, Zombie aqua (all from BioLegend) for 30 min at 4 °C. For intracellular cytokine staining, cells were restimulated with PMA (Sigma-Aldrich), ionomycin (Sigma-Aldrich), and GolgiPlug (BD Biosciences) for 4–6 h at 37 °C. Cyto-Fast Fix/Perm Buffer Set (BioLegend) or True-Nuclear Transcription Factor Buffer Set (BioLegend) and the mAbs specific for: IFN-γ (XMG1.2; BioLegend), IL-4 (11B11; BioLegend), FOXP3 (MF-14; BioLegend) IL-17 A

(TC11-18H10.1; BioLegend) and Ki-67 (16A8; BioLegend) were used for detecting intracellular transcription factors or cytokines according to the manufacturer's instruction as previously described. CellTrace Violet Cell Proliferation Kit (Invitrogen) was used for evaluation of cell division, and Cell Cycle Assay Solution Blue (Dojindo Laboratories) was used to measure the cell cycle according to the manufacturer's instructions. Cell proliferation and cell cycle were evaluated at day 2 under Th0 condition.

Human PBMCs were isolated using polymorphoprep and stained with the following hAbs specific for: CD3 (UCHT1), CD4 (OKT4), CD8 (QA18A37), CD25 (BC96), CD45RA (HI100), CD127 (A019D5), CD183 (CXCR3, G025H7), CD185 (CXCR5, J252D4), CD194 (CCR4, L291H4), CD196 (CCR6, G034E3) (all from BioLegend), and SYTOX Blue (Invitrogen) for 30 min at 4 °C. Stained cells were evaluated in FACS Verse (BD Biosciences) or Cytek Northern Lights (Cytek Biosciences) and analyzed with FlowJo V10 software.

2.8. Phagocytosis assay

Phagocytosis by BMDMs was observed for 6 h at 37 °C and imaged at 1 h intervals (Sartorius). Thresholds for calling pHrodo Green-positive events were set based on intensity measurements of pHrodo Green-labeled E.coli that lacked BMDMs, and the area of pHrodo Green-positive per $CD11b^+$ area were calculated using IncuCyte SX1.

2.9. Treg suppression assay

Tregs differentiated from naive$CD4^+$ T-cells as described above and Cell Trace-labeled $CD3^+$ T-cells from mouse spleen were co-cultured in the presence of anti-CD3 (1 μg/ml) and anti-CD28 (1 μg/ml) in respective ratios (Tregs: T-cells = 0:1, 1:1, 1:2, 1:4, 1:8). Cell division was assessed 48 h after starting co-culture. Percentage of suppression was calculated by ((% proliferating cells at 0:1 – % proliferating cells at each ratio) /% proliferating cells at 0:1) x 100 (%).

2.10. FAOBlue assay

FAOBlue (FDV-0033, Funakoshi) was dissolved in sterile-filtered DMSO and stored at −20 °C until use. T-cells under Th17 condition for 24 h were stained by 10 μM FAOBlue for 15 min. The fluorescence of FAOBlue was measured at excitation and emission wavelengths of 405 nm and 430–480 nm. Quantitative evaluation was performed using National Institutes of Health ImageJ imaging software.

2.11. RNA-sequencing

T-cells under Th17 conditions were treated with either vehicle or PEM for 48 h before harvest for RNA isolation. RNA-Seq was conducted by the Center of Medical Innovation and Translational Research, Osaka University, and by Macrogen Japan. The Illumina software package bcl2fastq was used for base calling. The raw reads were mapped to the house mouse reference genome sequence GRCm38 using TopHat (ver. 2.1.1) and Bowtie2 (ver. 2.3.4.1). Differential expression analysis was performed using the edgeR package (ver. 3.20.9). The fold change (FC) of gene expression between vehicle and PEM-treated groups was calculated. KEGG pathway enrichment analyses were conducted using the gseKEGG efunction in the clusterProfiler packag. An adjusted $P < 0.05$ was set as the cutoff criterion. A heatmap analysis was conducted using iDep.96 software. We defined differentially expressed genes (DEGs) according adjusted $P < 0.05$ and $|\log2FC| > 0.2$. The data discussed in this publication have been deposited in NCBI's Gene Expression Omnibus [18] and are accessible through GEO Series accession number GSE227073 (https://www.ncbi.nlm.nih.gov/geo/query/acc.cgi?acc=GSE227073).

2.12. Quantitative real-time PCR analysis

Total mRNA from T-cell was purified with RNeasy Mini Kit (QIAGEN) and reverse transcribed to generate cDNA (Invitrogen). Real-time SYBR-Green PCR analyses were performed using QuantoStudio7 (Applied Biosystems). Relative gene expression to Actinβ was evaluated by the comparative cycle threshold method. The primer sets are shown in Supplementary Table S1.

2.13. Histological analyses

Spinal cords and ears, skins were fixed in 4 % paraformaldehyde. Pathological changes were examined with hematoxylin and eosin (H&E) staining and luxol fast blue (LFB) staining. The sections were visualized by Nikon. Histopathological evaluation of IMQ-induced psoriasis-like skin inflammation was performed by two pathologists in a blinded fashion based on the Baker's scoring system [19], and the mean value was calculated.

2.14. Seahorse XF flux analyzer

Metabolic status such as mitochondrial oxygen consumption rate (OCR) were recorded using a 96-well XF Extracellular Flux Analyzer under the basal condition and in the presence of 1.5 μM oligomycin, 1.0 μM of trifluoromethoxy carbonylcyanide phenylhydrazone (FCCP), and 0.5 μM of rotenone and antimycin A (all from Agilent Technologies). Assay buffer was made of XF base medium with or without 2.0 mM glutamine in addition to 10 mM glucose and 1.0 mM sodium pyruvate (all from Agilent Technologies). Poly-D-lysine (Corning) was used for coating plates and 1.5×10^5 T-cells per well were seeded. To assess FAO, OCR was measured in the presence or absence of 5 μM etomoxir. In detail, basal respiration represents the mean value of OCR at three time points before oligomycin administration, and ATP-linked OCR represents the gap between basal OCR and the mean value of OCR at three time points after oligomycin administration. Maximal respiration is the mean OCR at three time points after FCCP administration. To calculate Δmaximal OCR, the maximal respiration was measured with and without etomoxir or glutamine, and differences were calculated between each of the wells measured at the same time. FAO: Δmaximal OCR = maximal OCR without etomoxir – maximal OCR with etomoxir. Glutaminolysis: Δmaximal OCR = maximal OCR with glutamine – maximal OCR without glutamine. In addition, to evaluate glycolysis, we performed Glycolytic Rate Assay and measured proton efflux rate (PER) in the presence of 0.5 μM of rotenone and antimycin A and 50 mM of 2-deoxyglucose (2-DG). Basal glycolysis was calculated by subtracting mitochondrial acidification from total proton efflux and compensatory glycolysis was measured after administration of rotenone and antimycin A. All other procedures were performed according to the manufacturer's instructions.

2.15. Statistical analysis

Parametric or non-parametric data was expressed as mean ± standard deviation or median with interquartile range. Two-tailed Student's *t*-test or Mann-Whitney test was used for analyzing difference between two groups. One-way ANOVA with Dunnett's multiple-comparison test was used for analyzing differences among three or more groups. For EAE model and psoriasis model, clinical scores and body weight changes of each group were compared using two-way analysis. *P* values <0.05 were considered statistically significant. Statistical analyses were performed by GraphPad Prism version 8.4.3 (GraphPad Software).

3. Results

3.1. Gender-independent effects of PEM in the alleviation of EAE are associated with specific reduction of Th17 cells

We first tested whether the ameliorative effects of EAE by PPARα agonists were reproducible, using a clinically relevant dose (0.1 mg/kg/day) of PEM administration in male and female mice. PEM certainly alleviated EAE in both clinical symptoms and weight loss, but unlikely with previous reports [13,14], these improvements were observed regardless of gender (Fig. 1A, B, S1A). Pathological findings and the number of spinal cord infiltrating cells ($CD45^+$ $CD11b^{mid}$ or $CD45^+$ $CD11b^-$ cells) confirmed the disease alleviation in PEM-treated group (Fig. 1C, D, S1B). Of particular significance, IFNγ-producing $CD4^+$ T-

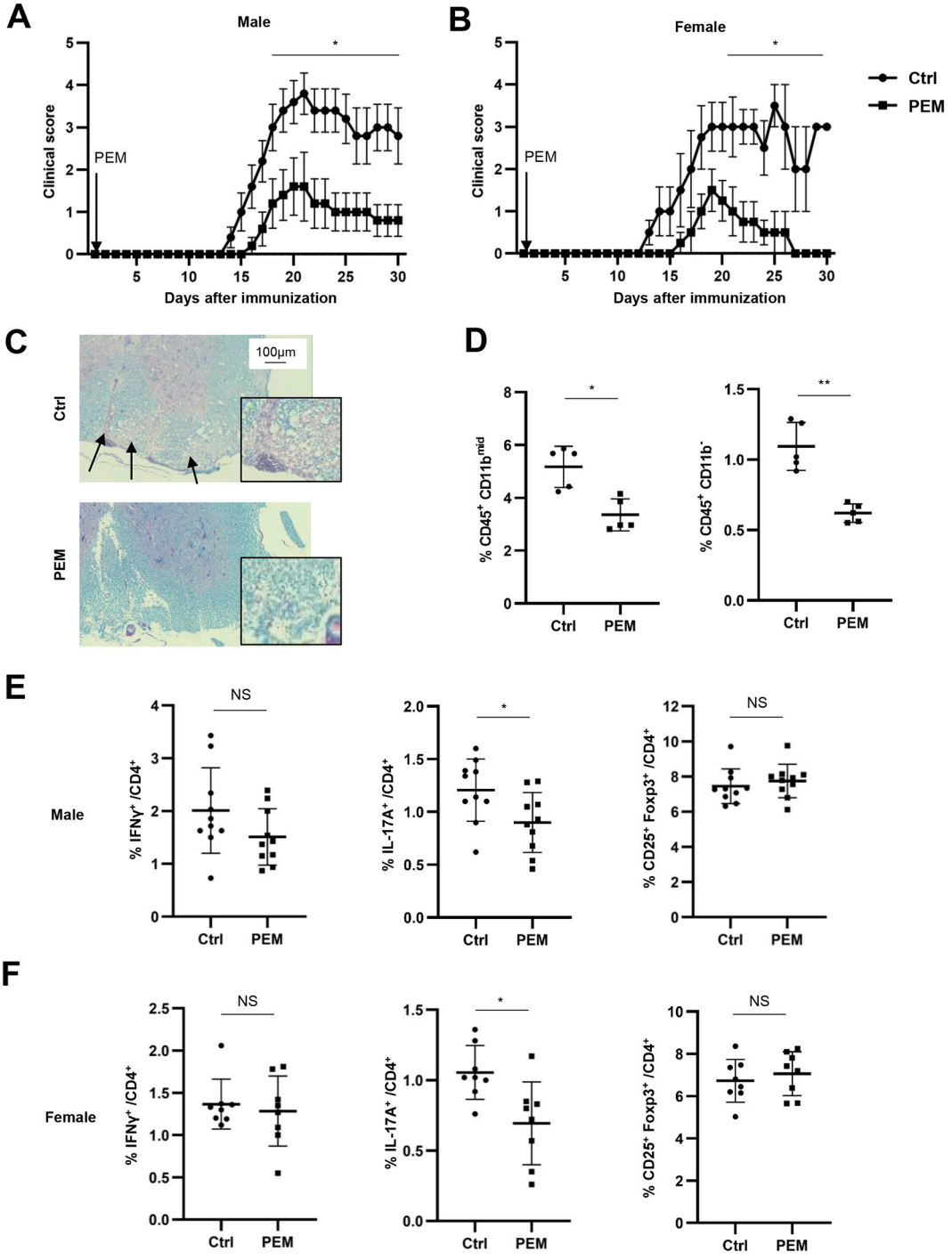

Fig. 1. Amelioration of EAE in PEM-treated mice.
(A, B) The mean (±s.e.m.) clinical scores were plotted at days after MOG immunization in male (A) and female (B) mice fed normal chow (round) or PEM containing chow (square) ($n = 5$ in each group, $^*P < 0.05$, two-way ANOVA with Bonferroni's post-test). (C) Representative luxol fast blue and eosin staining of spinal cord sections at the peak of clinical symptom (x40) in male EAE. Eosin-positive area with cell infiltration was observed (black arrows). (D) Percentages of $CD45^+$ $CD11b^{mid}$ (left) and $CD45^+$ $CD11b^-$ (right) cells from spinal cord were determined. (E, F) $IL17A^+$, $IFN\gamma^+$ and $CD25^+$ $Foxp3^+$ /$CD4^+$ T-cells in the inguinal lymph nodes of MOG-immunizued male (E) and female (F) mice at day 10. The bar graphs show the mean ± s.d. (n = 5–10, NS; Not Significant, $^*P < 0.05$, $^{**}P < 0.001$, two-tailed unpaired Student's t-test).

cells from the inguinal lymph node at day10, previously reported to be decreased by the treatment with conventional PPARα agonist, did not change by PEM; only IL-17-producing CD4$^+$ T-cells exhibited significant reduction with little increase of CD25$^+$ Foxp3$^+$ CD4$^+$ T-cells (Fig. 1E, S1C, S1D). This modulation in cytokine-producing cells was also observed in female (Fig. 1F). PEM administration after onset of the disease also ameliorated clinical symptoms, indicating the therapeutic benefit in the effector phase of autoimmunity (Fig. S1E). These observations prompted us to test the efficacy of PEM in another IL-17-related autoimmune disease.

3.2. PEM ameliorates imiquimod-induced dermatitis in female mice

To further investigate the gender-independent effects of PEM on IL-17, we used an imiquimod (IMQ)-induced psoriasiform dermatitis model in female mice, an IL-17-mediated inflammatory skin disease exhibiting significant symptoms in females [20,21]. PEM-treated group showed significant reduction of ear swelling as well as of pathological severity using Baker's scoring system (Fig. 2A, B). Skin inflammation evaluated by clinical score using PASI and pathological score also improved in PEM group (Fig. 2C, D). As similar to the previous results in EAE, reduction of IL-17-producing CD4$^+$ T-cells from the cervical lymph node was apparent in IMQ-induced dermatitis by PEM treatment, although IFNγ-producing or CD25$^+$ Foxp3$^+$ CD4$^+$ T-cells showed no

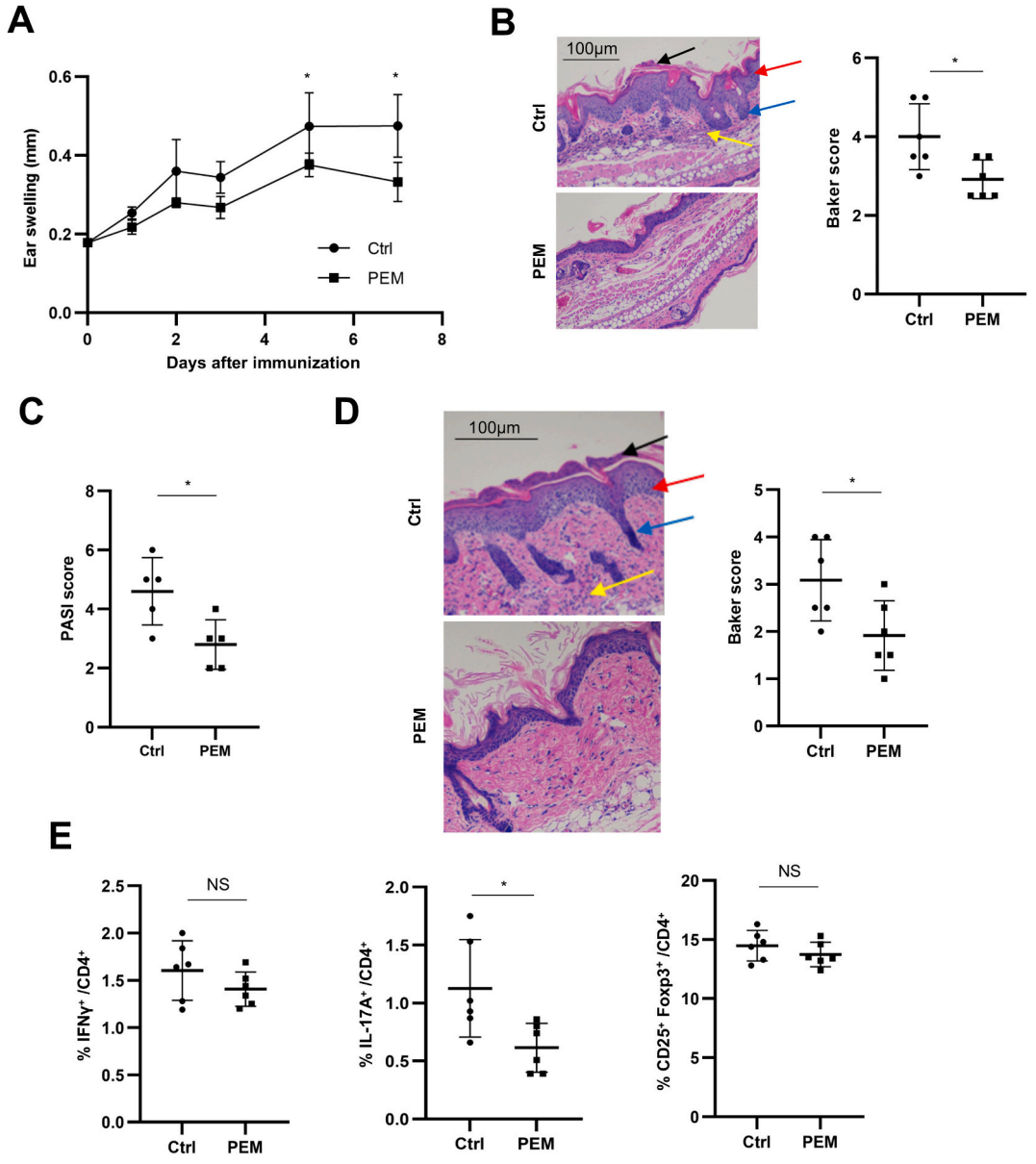

Fig. 2. Effect of PEM on psoriasis-like skin inflammation mice.
(A) The mean (±s.e.m.) thickness of the ear of each group was measured at the days after psoriasis-like skin inflammation was induced in female mice (n = 5 in each group, *P < 0.05, two-way ANOVA with Bonferroni's post-test). (B) The H&E staining of the earsf at day 7 (x100). Parakeratosis (black arrow), epidermal thickening (red arrow), rete ridges appearance (blue arrow) and lymphocytic infiltration (yellow arrow) are shown. Quantitative assessment of pathological score based on a Baker score system was performed (right). (C) The mean clinical scores for disease severity at day 7 were calculated using the clinical Psoriasis Area and Severity Index. (D) The H&E staining of the dorsal skin at day 7 (x100) is shown, as well as the ear staining shown above. Pathological score is based on a Baker score system (right). (E) Percentages of IL17 A$^+$, IFNγ$^+$ and CD25$^+$ Foxp3$^+$ in CD4$^+$ T-cell in the cervical lymph nodes of psoriasis-like skin inflammation mice at day 7 were evaluated. The bar graphs show the mean ± s.d. (n = 5–8, NS; Not Significant, *$P < 0.05$, **$P < 0.001$, two-tailed unpaired Student's *t*-test).

difference (Fig. 2E, S2A). In addition, we next used lupus-prone NZB/WF1 female mice to verify the IL-17-specific action of PEM. Although IL-17 is thought to play crucial roles in the pathogenesis of human SLE, the involvement of IL-17 in this mouse model of lupus appears to be minimal [22]. PEM did not prolong the induction of proteinuria or survival (Fig. S2B), and no significant changes were observed in anti-ds-DNA IgG titers (Fig. S2B). Collectively, our results suggest that PEM mitigates autoimmune inflammation irrespective of sex, by suppressing IL-17 but not IFNγ.

3.3. PEM alters Th17 cell differentiation and metabolism

RNAseq at 48 h under in vitro Th17-skewing condition in the presence of PEM revealed significant changes in Th17/Treg-related genes such as *Il17a, Il23r* and *Foxp3* (Fig. 3A, B), indicating the direct effects of PEM in lymphocytes. Th17 differentiation was substantially suppressed by only 1 nM of PEM supplementation, whereas both Th1 and Th2 cells were unaffected and Tregs were slightly increased (data not shown). As a result, Th17/Treg ratio decreased notably in proportion to the concentration of IL-6 in the presence of PEM (Fig. 3C). However, suppressive function of PEM-treated Tregs was not enhanced (Fig. S3 A). In addition to the change in Th17/Treg-related genes, PEM-treated T-cells increased genes related to fatty acid metabolisms such as *Cd36*, *Rxra* and *Acsl6*, while glutaminase 2 (*Gls2*), an enzyme for glutaminolysis, was downregulated. Other genes involved in the glycolysis, such as *Myc* and *Hif1a*, were also decreased, suggesting alterations on the metabolic programs of Th17 cells (Fig. 3A, B). To investigate how FAO is involved in these changes, we used etomoxir, an inhibitor of carnitine palmitoyltransferase 1 A (CPT1a) which is a rate-limiting enzyme for mitochondrial FAO as a target of PPARα. As a result, etomoxir reversed the inhibitory effect of PEM, indicating that FAO played critical roles in PEM-mediated suppression of Th17 cells (Fig. 3D, S3B). On the other hand, Treg, in which FAO is the main metabolic pathway [9], was hardly promoted in differentiation by PEM, but was certainly inhibited by etomoxir (Fig. S3C). We further analyzed changes in gene expressions of PEM- and PEM plus etomoxir-treated Th17 cells. While genes related to FAO (*Cpt1a*, *Acadl*, *Acox1*) were increased by PEM as expected, it is notable that those to glycolysis (*Gapdh*, *Hk2*), glutaminolysis (*Gls*, *Gls2*, *Glud1*) and Th17 differentiation (*Rorc*) were significantly decreased. Genes involved in FAS (*Acaca*, *Fasn*) were not affected (Fig. 3E). Reduced glutaminolysis is reflected in the elevated glutamine concentration from the medium of PEM-treated T-cells compared to the control (Fig. 3F). More importantly, when FAO was inhibited by etomoxir, gene expressions related to glycolysis and glutaminolysis were totally restored. PEM-induced fatty acid transporter Cd36 and acyl-CoA oxidase 1 (*Acox1*) were not reversed by etomoxir, indicating that PPARα-target genes related to non-mitochondrial FAO were unaffected by etomoxir treatment (Fig. 3E).

3.4. Differential effects of PPARα agonists on T-cell differentiation and cellular activity

Fenofibrate (FEN), a conventional PPARα agonist, was also reported to inhibit Th17 differentiation at 10 μM, a clinically relevant concentration [23]. Therefore, we compared PEM and FEN to determine how their effects on T-cells differ according to PPARα selectivity. Since FEN did not suppress Th17 differentiation at the dose of 1 μM but significantly at 10 μM (Fig. S4 A), we performed the following experiments with 10 μM of FEN and10 nM of PEM. In contrast to PEM, the inhibitory effect of FEN was not reversed by etomoxir (Fig. 4A). Consistent with previous reports, IFN-γ producing cells were apparently reduced by FEN (Fig. 4B), however, we found that the number of live cells were significantly decreased in 10 μM of FEN-treated effector T-cells (Fig. 4C). FEN-treated T-cells showed tendency of G0/G1 arrest upon stimulation (Fig. 4D), resulting in the suppression of cell division (Fig. 4E, S4B). Notably, FEN increased 7-AAD^{+} dead cells under both Th1 and Th17 condition (Fig. 4F), suggesting that FEN inhibits T-cell growth leading to cell death whereas PEM exclusively suppresses Th17 differentiation. Decreased expression of genes related to glycolysis, glutaminolysis and FAS was not restored by etomoxir treatment (Fig. S4C). These results suggest that PEM-mediated activation of PPARα could interfere with Th17-skewing metabolic programs such as glycolysis and glutaminolysis in an FAO-dependent manner, while FEN-mediated suppression of Th17 might be FAO-independent inhibition of cell growth.

We next examined whether PPARα activation could also act on macrophages derived from bone marrow. Glycolysis and FAS are active in inflammatory macrophage (M1), while anti-inflammatory macrophage (M2) is more dependent on FAO [24]. Reflecting the dominant expression of PPARγ rather than PPARα in macrophage [12], PPARγ agonist pioglitazone (PIO) consistently upregulated genes related to fatty acid metabolism (*Cpt1a*, *Acadl*, *Cd36* and *Acox1*) (Fig. S4D). Evaluation of macrophage polarization showed that genes related to M1 polarization (*Nos2*, *Cd86*) were downregulated (Fig. S4E), whereas genes related to M2 polarization (*Arg1*, *Ym1*) were upregulated by PIO (Fig. S4F), as previously reported [25]. In addition to the modulation of cytokine production such as suppression of TNFα and IL-1β (Fig. S4G), and elevation of IL-10 (Fig. S4H), phagocytosis was also inhibited by PIO (Fig. S4I). In contrast, PEM did not change gene expressions for fatty acid metabolism, genes for polarization, cytokine productions or phagocytic function (Fig. S4D—I). Taken together, PEM directly targets T-cells and not macrophages to shift the Th17/Treg balance, while FEN affects T-cell viability through PPARα-independent mechanisms.

3.5. Mitochondrial FAO-dependent alterations of metabolic program by PEM restrain Th17 cell differentiation

Enhancement of FAO in PEM-treated Th17 cells was visualized using fluorescence-based FAO detection reagent, FAOblue (Fig. S5 A) [26]. To further assess the metabolic reprogramming of PEM-treated Th17 cells, oxygen consumption rate (OCR) and proton efflux rate (PER) were measured by extracellular flux analyzer. While basal, maximal and ATP-linked OCR (energy production by OXPHOS) were not changed, glycolysis evaluated by PER was reduced in PEM-treated Th17 cells (Fig. 5A, B, S5B). Considering that glutamine metabolism is essential for Th17 cell differentiation and function (Fig. S5C), we investigated the bias in energy production by PEM in Th17 cells. The dependence of energy production on FAO and glutaminolysis was examined by etomoxir and deprivation of glutamine, respectively. The gap in OCR (ΔOCR) was calculated during maximal respiration influenced by oxidation in the mitochondria through the TCA cycle such as FAO and amino acid metabolism, especially in cells with increased energy demand (Fig. 5C, D) [27]. The ΔOCRs resulting from these treatments were regarded as the energy production dependent on each metabolic pathway. In PEM-treated Th17 cells, energy production within the mitochondria was deduced to be highly dependent on FAO (Fig. 5C), while glutamine dependency was significantly reduced (Fig. 5D). These findings suggest that PEM alters the metabolic program of Th17 cells, shifting from glutamine to fatty acid metabolism for energy supply, and therefore this transformation implies a substantial decrease in the functional capacity of Th17 cells. In contrast, FEN decreased glycolysis, glutaminolysis and OXPHOS (Fig. 5A-D, S5B).

Previous study has reported a substantial role for pathogenic Th17 differentiated in the presence of IL-1β, IL-6 and IL-23 in the pathogenesis of EAE [28]. Therefore, we added the examination about pathogenic Th17. Similar to Th17 differentiated in the presence of TGFβ and IL-6, polarization of pathogenic Th17 was surppressed by PEM (Fig. S5D), with an increase in FAO and a decrease in glutamine metabolism while maintaining mitochondrial ATP production (Fig. S5E, S5F). In addition, this inhibitory effect by PEM was FAO-dependent (Fig. S5G).

In summary, metabolic profiles were obviously different between PEM and FEN-treated cells (Fig. 5E). While mitochondrial ATP production is maintained in PEM-treated Th17 cells, all metabolic processes

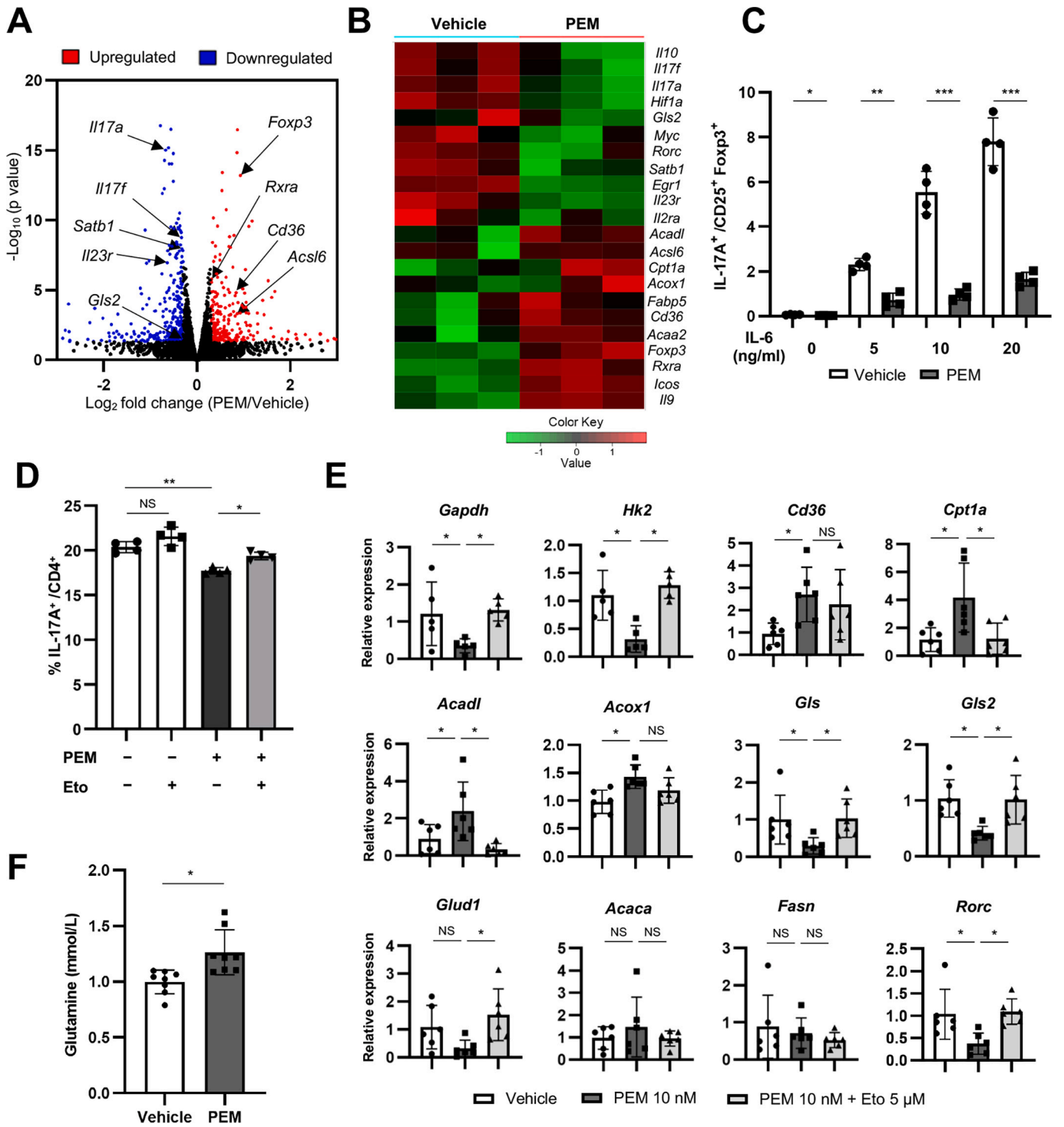

Fig. 3. Direct effects of PEM on T-cell differentiation and metabolism.
(A, B) RNAseq of T cells cultured for 48 h in Th17-skewing condition with or without PEM. (A) Volcano plot of differential gene expression identified between the PEM-treated cells and controls. The genes upregulated in PEM-treated cells are shown in red, and the genes downregulated are shown in blue. (B) Heat map showing the relative expression of genes related to Th17, Treg and metabolism. The upregulated genes are shown in red, and the downregulated genes are shown in green. (C) Naïve $CD4^+$ T-cells were cultured under Th17 condition in medium containing the indicated doses of IL6 (0–20 ng/ml). IL-17 A^+ /$CD25^+$ $Foxp3^+$ ratio was evaluated. (D) IL-17 A^+ $CD4^+$ T-cells were measured at 96 h after Th17-skewing conditions with drugs as indicated. (E) The relative mRNA expression to *Actinβ* were evaluated by quantitative RT-PCR at 48 h after Th17 condition. (F) The supernatant glutamine concentrations were compared in two groups at 96 h under Th17 condition. The bar graphs show the mean ± s.d. ($n = 4$–8, NS; Not Significant, $^*P < 0.05$, $^{**}P < 0.001$, $^{***}P < 0.0001$, two-tailed unpaired Student's t-test or one-way ANOVA with Dunnett's multiple-comparison test).

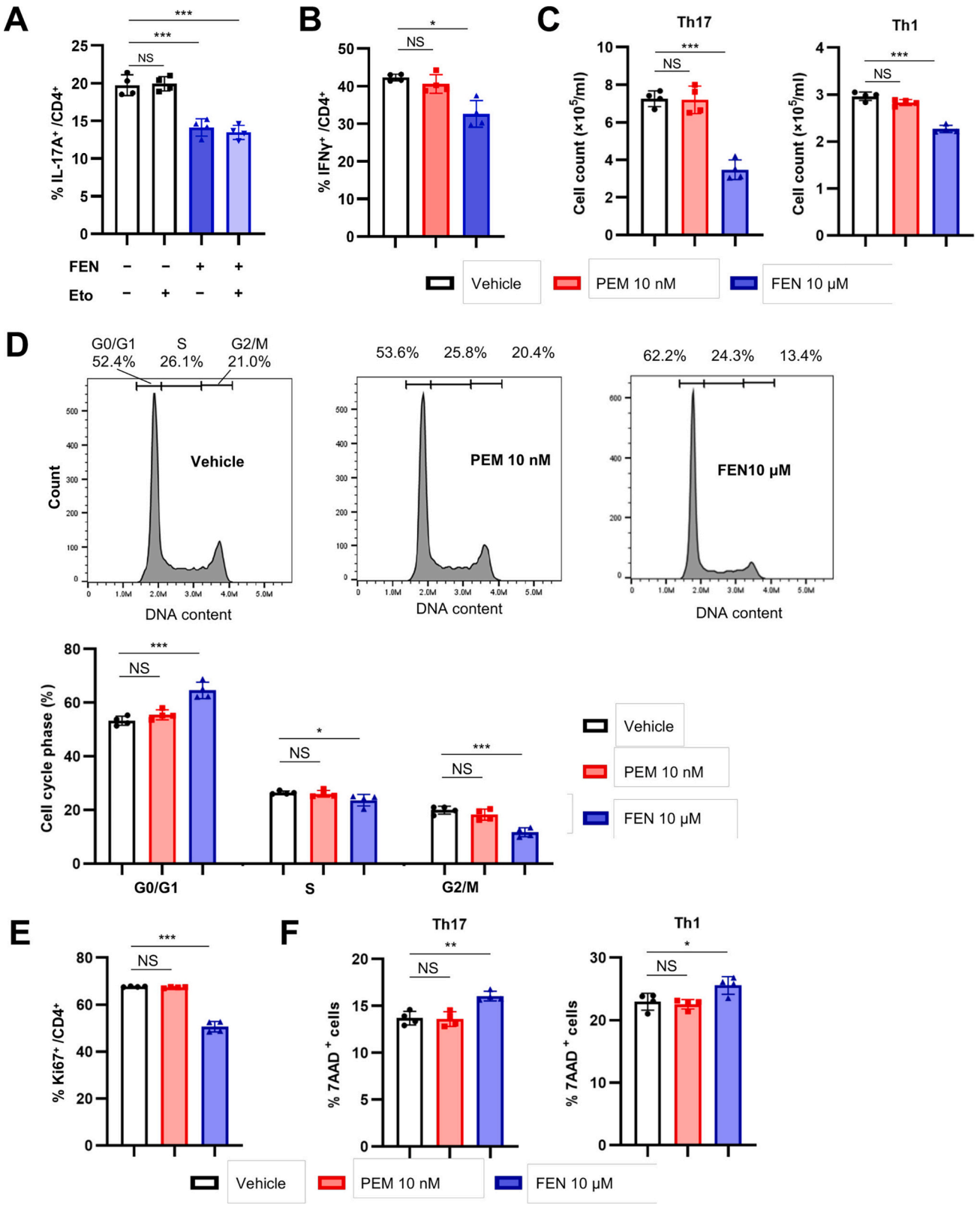

Fig. 4. Differential effects of PPARα agonists on T-cells.
(A) Naïve $CD4^+$ T-cells were cultured under Th17 conditions and DMSO or FEN was added with or without etomoxir on day 0. Percentage of IL-17 A^+ cells /$CD4^+$ T-cells were measured by flow cytometry on day 4. (B, C) IFNγ $^+$ cells /$CD4^+$ T-cells (B) under Th1 condition, and number of $CD4^+$ T-cells (C) under Th17 or Th1 condition were measured by flow cytometry on day 4. (D, E) Cells in G0/G1, S, or G2/M phase with representative histogram (D) and that of Ki-67$^+$ cells /$CD4^+$ T-cells (E) were compared at 48 h under Th0 condition. (F) $7AAD^+$ cells under Th17 and Th1 condition. Data except for A and B are representative of at least two independent experiments. The bar graphs show the mean ± s.d. ($n = 4$, NS; Not Significant, $^*P < 0.05$, $^{**}P < 0.001$, $^{***}P < 0.0001$, one-way ANOVA with Dunnett's multiple-comparison test).

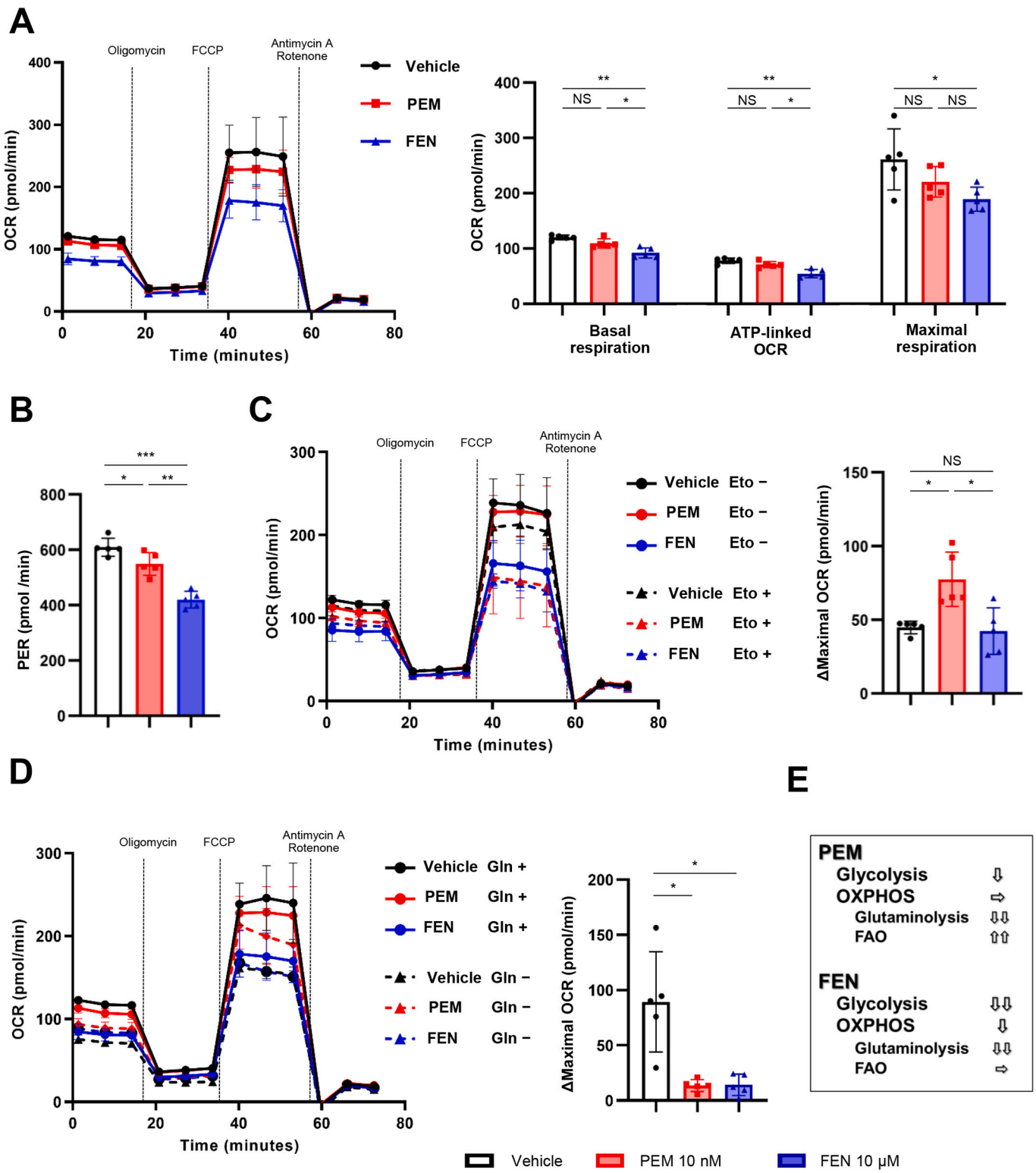

Fig. 5. FAO-dependent metabolic modification by PEM different from FEN.
(A-E) Oxygen consumption rate (OCR) and extracellular acidification rate (ECAR) of Th17 cells were measured by extracellular flux analyzer. (A) Basal, ATP-linked and maximal OCR, and (B) basal glycolysis evaluated by proton efflux rate (PER) were compared in three groups. (C) The gap in maximal OCR (Δmaximal OCR) was calculated with or without etomoxir. The comparison of OCR measured with (dotted) or without (solid) etomoxir is shown in vehicle (black), PEM-treated (red) and FEN-treated Th17 cells (blue). (D) ΔMaximal OCR was calculated with (solid) or without (dotted) glutamine. The comparison of OCR measured with or without glutamine is shown in vehicle (black), PEM-treated (red) and FEN-treated Th17 cells (blue). (E) The summary of alteration in metabolic status. Results are representative of at least two independent experiments. The bar graphs show the mean ± s.d. (n = 4–6, NS; Not Significant, *$P < 0.05$, **$P < 0.001$, ***$P < 0.0001$, one-way ANOVA with Tukey's multiple-comparison test).

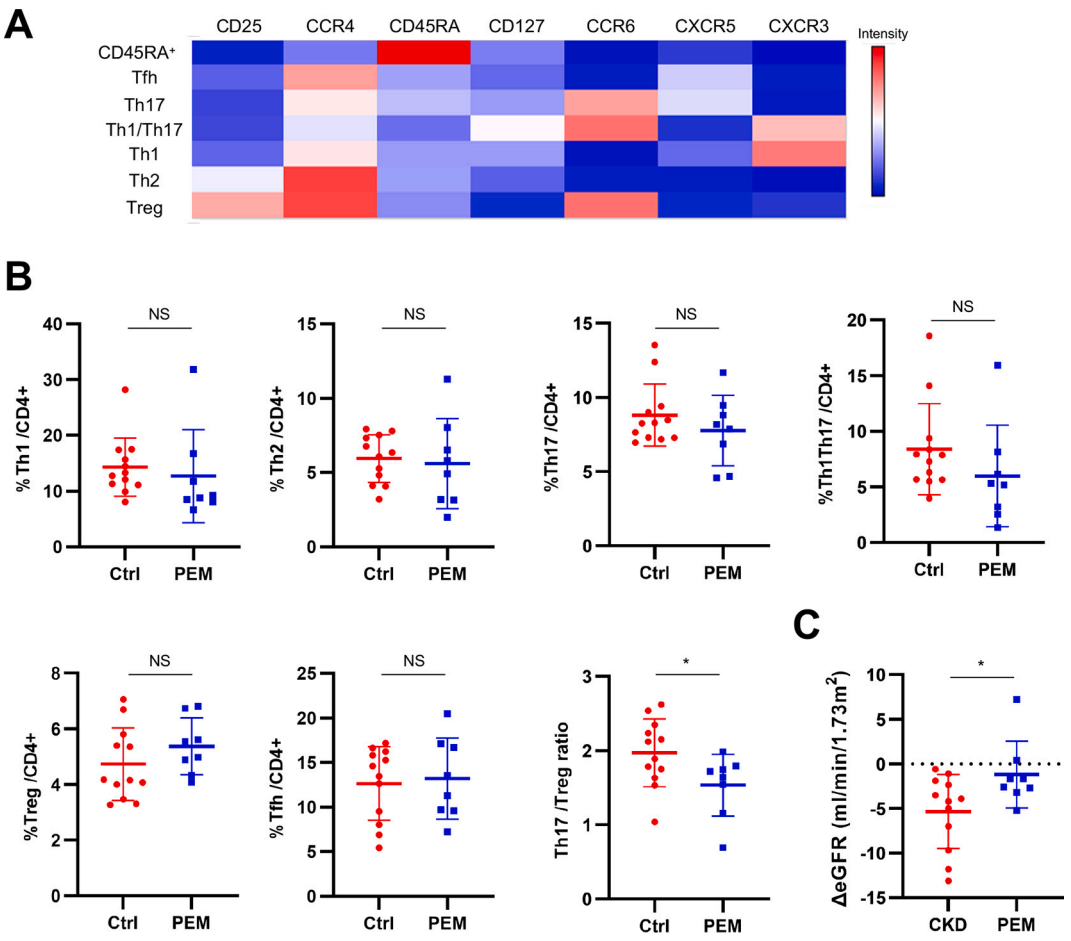

Fig. 6. Shift in Th17/Treg balance of peripheral lymphocytes from CKD patients treated with PEM.
(A) Heatmap of clusters among $CD4^+$ T-cells classified based on combinations of selected surface markers by flow cytometry. (B) Percentages of Th1, Th2, Th17, Th1/Th17, Treg and Tfh /$CD4^+$ T-cells and ratio of Th17/Treg were measured in patients treated without PEM (Ctrl, red) and with PEM (PEM, blue). (C) Comparison of ΔeGFR in one year between the two groups. The bar graphs show the mean ± s.d. (NS, Not Significant, *P < 0.05, two-tailed unpaired Student's *t*-test).

suppressed in FEN-treated cells might be unable to meet the increased energy demand according to activation, leading to cell death.

3.6. Modified Th17/Treg balance in patients treated with PEM

Th17 cells were reported to be increased in patients with advanced chronic kidney disease (CKD) [29]. Since PEM is now available for use in advanced CKD patients in Japan, we examined the difference in T-cells between our patients treated with and without PEM. Lymphocytes from peripheral blood were divided into several clusters using flow cytometry by staining for cell surface markers and $CD4^+$ T-cells isolated from our patients were classified according to their staining patterns. As previously reported [30,31], we defined these clusters as $CD4^+$ $CD45RA^+$ cells, Tfh ($CD4^+$ $CD25^-$ $CXCR3^-$ $CXCR5^+$), Th17 ($CD4^+$ $CD25^-$ $CCR6^+$ $CXCR3^-$ $CXCR5^-$), Th1/17 ($CD4^+$ $CD25^-$ $CCR6^+$ $CXCR3^+$ $CXCR5^-$), Th1 ($CD4^+$ $CD25^-$ $CCR6^-$ $CXCR3^+$ $CXCR5^-$), Th2($CD4^+$ $CD25^-$ $CCR4^+$ $CCR6^-$ $CXCR3^-$ $CXCR5^-$) and Treg ($CD4^+$ $CD25^+$ $CD127^-$ $CCR4^+$) (Fig. 6A, S6). Patient characteristics such as age, gender, estimated glomerular filtration rate, C-reactive protein, and urine protein/urine creatinine ratio did not differ between the two groups (Table S2). While there was no significant difference in percentage of each T-cell subset, Th17/Treg ratio was significantly lower in the PEM group as compared in control CKD patient group (Fig. 6B). Furthermore, evaluation for clinical outcome showed a milder decline of eGFR at one year in the PEM group (Fig. 6C).

4. Discussion

We demonstrated that PEM-mediated specific PPARα activation alleviated IL-17-related autoimmune diseases. Although enhanced PPARα expression in male was indicated to play its substantial role [32], our findings that PEM ameliorated EAE in both male and in female, suggesting the effect dependent on the high affinity of PEM for PPARα rather than the expression levels of PPARα. On the other hand, PEM did not ameliorate the disease progression of lupus-prone NZB/WF1 mice. The involvement of IL-17 in this model might be limited, which is explained from the fact that disease progression of NZB/WF1 mice was unaffected in IL-17-deficiency and that IL-17 was not detected in injured kidneys [22,33]. Moreover, the fact that even the percentage of Th17 in the spleen of NZB/WF1 mice was not significantly reduced by PEM (data not shown) may be due to heterogeneity of Th17 cells. It is noted that Th17 has diverse functions, such as maintenance of homeostasis and inflammation [34]. In our study, PEM suppressed pathogenic Th17 cell differentiation as well as homeostatic Th17 cells. Although it is already known that pathogenic Th17 cells are involved in the development of EAE and psoriasis, those in SLE is still controversial [35]. However, IL-17 remains significant in SLE progression, and there still exists the potential target for some disease phenotype [36,37].

Manipulation of the metabolic pathway to modify the Th17/Treg balance is reported to be a potentially feasible solution for the treatment of autoimmune disease [38]. In this study, we hypothesized that Th17 cells could be affected by the upregulation of mitochondrial FAO, which has been considered to be dispensable for its differentiation [39]. PEM-

induced increase in mitochondrial FAO such as *Cpt1a* and *Acadl* and decrease in glycolysis and glutaminolysis were both reversed by etomoxir, which suggests that PEM-mediated inhibition of Th17 cells is based on FAO-dependent alteration of metabolic program in T-cells. These results suggest that the excess, not the deficiency, of *Cpt1a* affects Th17 differentiation. In contrast, PEM had little effect on macrophages, where PPARγ expression is predominant rather than PPARα. This provides convincing evidence for metabolic regulation of Th17 cells via PPARα activation. Since Th17 differentiated in the presence of TGFβ and IL-6 is reported to be more FAO-dependent than pathogenic Th17, it is necessary to examine the effects on pathogenic Th17, which is less dependent on FAO [40]. Inhibition of differentiation via metabolic alterations was also observed for pathogenic Th17, which may contribute to the amelioration of autoimmune diseases and further investigation is required.

We also addressed the pharmacobiological differences between PEM and conventional PPARα agonist. FEN requires more than 1000 times higher concentration than that of PEM to achieve the same level of PPARα activity [41]. Our results demonstrate that FEN deprives energy even at a dose of clinical relevance, by broadly restraining cellular metabolism, which causes impairment of T-cell proliferation and of viability. These observations could explain differences between PPARα-mediated and non-PPARα-mediated effects on immune responses.

Although both fibrates restrain Th17 cells, it is of interest that FEN was likely to act as a metabolic inhibitor, whereas PEM worked as an accelerator of fatty acid metabolisms. The pharmacological action of FEN may be reflected in some recent evidence of its potential as an anticancer drug, along with its immunosuppressive function [42,43]. Similarly, metabolic interventions have been explored for the treatment of autoimmune diseases. In a mouse lupus model, clinical symptoms were alleviated by inhibiting glycolysis with 2-DG and OXPHOS with metformin [44], and by inhibiting glucose transporter [45]. EAE has been shown to be ameliorated by glutaminase inhibitor BPTES and inhibitors of FAS [46,47]. These targets inhibit metabolic signals that are critical to cell proliferation, however, administration of effective dosages may also affect somatic cellular activity. In fact, clinical trials of 2-DG have been conducted for cancer treatment, but serious side effects such as seizures occurred at therapeutic doses and were terminated [48]. Enzyme inhibitors for FAS have undergone clinical trials for cancer and non-alcoholic fatty liver disease, however, some were abandoned because of severe adverse effects or others are still under investigation [49,50]. Thus far, clinical trials of metabolite modulators for autoimmune diseases have not been conducted. Given these circumstances, the significance of this study underlies in the fact that PEM, unlike FEN, was able to maintain energy production by decreasing glycolysis and glutaminolysis via upregulation of FAO and modify the Th17/Treg balance without affecting cell viability, which may facilitate its clinical application in these diseases.

Clinical availability of PEM in Japan enabled us to validate its efficacy on patients. Despite the fact that most of our patients had impaired renal function and required dose reductions, Th17/Treg balance was modified and rate of eGFR decline was smaller in patients receiving PEM. It has been noted that IL-17 is involved in the development of diseases that cause AKI and CKD, such as glomerulonephritis, renal ischemia, diabetic nephropathy, hypertension, and atherosclerosis [51]. In human, different from mice, PEM did not significantly reduce Th17, but altered Th17/Treg balance. However, considering the degree of change in Th17 and Treg, the reduction in Th17 might have contributed to the significant difference in Th17/Treg ratio. This is likely due to variations in the underlying kidney diseases or to differences in the dosage and period of PEM. Particularly, PEM is only allowed in lower doses (0.1 or 0.2 mg/day) for CKD patients than in non-CKD patients (maximum 0.4 mg/day). Future studies are needed to establish the correlation between the dose of PEM in mice and human. It should also be noted that T-cell subsets were classified by only surface markers, and therefore do not necessarily refer to each cytokine-producing cell. Although clinical trials are also required in the future, PEM may inhibit CKD progression through the modification of Th17/Treg balance, which may expand its availability for CKD patients.

In clinical settings, lipid metabolism is closely associated with autoimmune diseases. It has been noted that patients with multiple sclerosis (MS) tend to have disrupted lipid metabolism and are more likely to have dyslipidemia as a complication [52,53]. As well, patients with psoriasis have a high prevalence of metabolic diseases such as diabetes, hypertension, dyslipidemia and obesity, indicating a strong association between psoriasis and metabolic syndrome [54,55]. Therefore, the use of PEM, a metabolic modifying drug, for these autoimmune diseases is reasonable and may help in future treatment. Furthermore, while strong immunosuppressive effects are concerned with FEN, PEM was not associated with an increase in the total incidence of serious adverse events, as reported in the PROMINENT study [16]. Currently, PEM is only available for dyslipidemia, which limits the opportunity to use it for patients with MS and psoriasis. From the perspective of drug repositioning, selective PPARα activator could be a viable option for the treatment of autoimmune diseases beyond its conventional indications.

5. Conclusions

Our findings provide evidence that selective PPARα activation by PEM modifies the metabolic programs of Th17 cells via FAO enhancement and could be an effective target for the treatment of autoimmune diseases.

CRediT authorship contribution statement

Satoshi Masuyama: Writing – review & editing, Writing – original draft, Methodology, Investigation, Conceptualization. **Masayuki Mizui:** Writing – review & editing, Writing – original draft, Supervision, Methodology, Investigation, Funding acquisition, Formal analysis, Conceptualization. **Masashi Morita:** Writing – review & editing, Methodology, Investigation. **Takatomo Shigeki:** Writing – review & editing, Methodology, Investigation. **Hisakazu Kato:** Writing – review & editing, Resources. **Takeshi Yamamoto:** Writing – review & editing. **Yusuke Sakaguchi:** Writing – review & editing. **Kazunori Inoue:** Writing – review & editing. **Tomoko Namba-Hamano:** Writing – review & editing. **Isao Matsui:** Writing – review & editing. **Tatsusada Okuno:** Writing – review & editing. **Ryohei Yamamoto:** Writing – review & editing. **Seiji Takashima:** Writing – review & editing, Resources. **Yoshitaka Isaka:** Writing – review & editing, Supervision.

Declaration of competing interest

All authors do not have any other financial support which could create a potential conflict of interest or the appearance of a conflict of interest concerning the work in the manuscript.

Data availability

The data reported in this paper is available on request.

Acknowledgments

The authors would like to thank Naoko Horimoto for her technical assistance. We are also grateful to CentMeRE and CoMIT Omics Center, Osaka University Graduate School of Medicine, for providing technical support. This work was supported by Japan Society for the Promotion of Science, Grant-in-Aid for Scientific Research(C) 22K08562 (M. Mizui). Pemafibrate was provided by Kowa Company Ltd.

Appendix A. Supplementary data

Supplementary data to this article can be found online at https://doi.org/10.1016/j.clim.2024.110357.

References

[1] M.D. Buck, D. O'Sullivan, E.L. Pearce, T cell metabolism drives immunity, J. Exp. Med. 212 (2015) 1345–1360, https://doi.org/10.1084/jem.20151159.

[2] R. Wang, C.P. Dillon, L.Z. Shi, S. Milasta, R. Carter, D. Finkelstein, et al., The transcription factor Myc controls metabolic reprogramming upon T lymphocyte activation, Immunity 35 (2011) 871–882, https://doi.org/10.1016/j.immuni.2011.09.021.

[3] Z. Yang, E.L. Matteson, J.J. Goronzy, C.M. Weyand, T-cell metabolism in autoimmune disease, Arthritis Res. Ther. 17 (2015) 29, https://doi.org/10.1186/s13075-015-0542-4.

[4] C.H. Patel, R.D. Leone, M.R. Horton, J.D. Powell, Targeting metabolism to regulate immune responses in autoimmunity and cancer, Nat. Rev. Drug Discov. 18 (2019) 669–688, https://doi.org/10.1038/s41573-019-0032-5.

[5] V.A. Gerriets, R.J. Kishton, A.G. Nichols, A.N. Macintyre, M. Inoue, O. Ilkayeva, et al., Metabolic programming and PDHK1 control CD4+ T cell subsets and inflammation, J. Clin. Invest. 125 (2015) 194–207, https://doi.org/10.1172/JCI76012.

[6] A.N. Macintyre, V.A. Gerriets, A.G. Nichols, R.D. Michalek, M.C. Rudolph, D. Deoliveira, et al., The glucose transporter Glut1 is selectively essential for CD4 T cell activation and effector function, Cell Metab. 20 (2014) 61–72, https://doi.org/10.1016/j.cmet.2014.05.004.

[7] M. Kono, N. Yoshida, K. Maeda, G.C. Tsokos, Transcriptional factor ICER promotes glutaminolysis and the generation of Th17 cells, Proc. Natl. Acad. Sci. USA 115 (2018) 2478–2483, https://doi.org/10.1073/pnas.1714717115.

[8] M.O. Johnson, M.M. Wolf, M.Z. Madden, G. Andrejeva, A. Sugiura, D.C. Contreras, et al., Distinct regulation of Th17 and Th1 cell differentiation by Glutaminase-dependent metabolism, Cell 175 (2018) 1780–1795 e1719, https://doi.org/10.1016/j.cell.2018.10.001.

[9] G.A. Gualdoni, K.A. Mayer, L. Goschl, N. Boucheron, W. Ellmeier, G.J. Zlabinger, The AMP analog AICAR modulates the Treg/Th17 axis through enhancement of fatty acid oxidation, FASEB J. 30 (2016) 3800–3809, https://doi.org/10.1096/fj.201600522R.

[10] H. Shi, H. Chi, Metabolic control of Treg cell stability, Plasticity, and Tissue-Specific Heterogeneity, Front. Immunol. 10 (2019) 2716, https://doi.org/10.3389/fimmu.2019.02716.

[11] R.A. Daynes, D.C. Jones, Emerging roles of PPARs in inflammation and immunity, Nat. Rev. Immunol. 2 (2002) 748–759, https://doi.org/10.1038/nri912.

[12] D.C. Jones, X. Ding, R.A. Daynes, Nuclear receptor peroxisome proliferator-activated receptor alpha (PPARalpha) is expressed in resting murine lymphocytes. The PPARalpha in T and B lymphocytes is both transactivation and transrepression competent, J. Biol. Chem. 277 (2002) 6838–6845, https://doi.org/10.1074/jbc.M106908200.

[13] A.E. Lovett-Racke, R.Z. Hussain, S. Northrop, J. Choy, A. Rocchini, L. Matthes, et al., Peroxisome proliferator-activated receptor alpha agonists as therapy for autoimmune disease, J. Immunol. 172 (2004) 5790–5798, https://doi.org/10.4049/jimmunol.172.9.5790.

[14] S.E. Dunn, S.S. Ousman, R.A. Sobel, L. Zuniga, S.E. Baranzini, S. Youssef, et al., Peroxisome proliferator-activated receptor (PPAR)alpha expression in T cells mediates gender differences in development of T cell-mediated autoimmunity, J. Exp. Med. 204 (2007) 321–330, https://doi.org/10.1084/jem.20061839.

[15] S. Yamashita, M. Rizzo, T.C. Su, D. Masuda, Novel selective PPARalpha modulator Pemafibrate for dyslipidemia, nonalcoholic fatty liver disease (NAFLD), and atherosclerosis, Metabolites 13 (2023), https://doi.org/10.3390/metabo13050626.

[16] A. Das Pradhan, R.J. Glynn, J.C. Fruchart, J.G. MacFadyen, E.S. Zaharris, B. M. Everett, et al., Triglyceride lowering with Pemafibrate to reduce cardiovascular risk, N. Engl. J. Med. 387 (2022) 1923–1934, https://doi.org/10.1056/NEJMoa2210645.

[17] S. Ida, R. Kaneko, K. Murata, Efficacy and safety of pemafibrate administration in patients with dyslipidemia: a systematic review and meta-analysis, Cardiovasc. Diabetol. 18 (2019) 38, https://doi.org/10.1186/s12933-019-0845-x.

[18] R. Edgar, M. Domrachev, A.E. Lash, Gene expression omnibus: NCBI gene expression and hybridization array data repository, Nucleic Acids Res. 30 (2002) 207–210, https://doi.org/10.1093/nar/30.1.207.

[19] D.Q. Luo, H.H. Wu, Y.K. Zhao, J.H. Liu, F. Wang, Original research: different imiquimod creams resulting in differential effects for imiquimod-induced psoriatic mouse models, Exp. Biol. Med. (Maywood) 241 (2016) 1733–1738, https://doi.org/10.1177/1535370216647183.

[20] A. Ueyama, M. Yamamoto, K. Tsujii, Y. Furue, C. Imura, M. Shichijo, et al., Mechanism of pathogenesis of imiquimod-induced skin inflammation in the mouse: a role for interferon-alpha in dendritic cell activation by imiquimod, J. Dermatol. 41 (2014) 135–143, https://doi.org/10.1111/1346-8138.12367.

[21] P. Alvarez, L.E. Jensen, Imiquimod treatment causes systemic disease in mice resembling generalized pustular psoriasis in an IL-1 and IL-36 dependent manner, Mediat. Inflamm. 2016 (2016) 6756138, https://doi.org/10.1155/2016/6756138.

[22] T. Schmidt, H.J. Paust, C.F. Krebs, J.E. Turner, A. Kaffke, S.B. Bennstein, et al., Function of the Th17/interleukin-17A immune response in murine lupus nephritis, Arthritis Rheum. 67 (2015) 475–487, https://doi.org/10.1002/art.38955.

[23] Z. Zhou, W. Sun, Y. Liang, Y. Gao, W. Kong, Y. Guan, et al., Fenofibrate inhibited the differentiation of T helper 17 cells in vitro, PPAR Res. 2012 (2012) 145654, https://doi.org/10.1155/2012/145654.

[24] A. Batista-Gonzalez, R. Vidal, A. Criollo, L.J. Carreno, New insights on the role of lipid metabolism in the metabolic reprogramming of macrophages, Front. Immunol. 10 (2019) 2993, https://doi.org/10.3389/fimmu.2019.02993.

[25] Q. Yao, J. Liu, Z. Zhang, F. Li, C. Zhang, B. Lai, et al., Peroxisome proliferator-activated receptor gamma (PPARgamma) induces the gene expression of integrin alpha(V)beta(5) to promote macrophage M2 polarization, J. Biol. Chem. 293 (2018) 16572–16582, https://doi.org/10.1074/jbc.RA118.003161.

[26] S. Uchinomiya, N. Matsunaga, K. Kamoda, R. Kawagoe, A. Tsuruta, S. Ohdo, et al., Fluorescence detection of metabolic activity of the fatty acid beta oxidation pathway in living cells, Chem. Commun. (Camb.) 56 (2020) 3023–3026, https://doi.org/10.1039/c9cc09993j.

[27] P. Marchetti, Q. Fovez, N. Germain, R. Khamari, J. Kluza, Mitochondrial spare respiratory capacity: mechanisms, regulation, and significance in non-transformed and cancer cells, FASEB J. 34 (2020) 13106–13124, https://doi.org/10.1096/fj.202000767R.

[28] C.L. Langrish, Y. Chen, W.M. Blumenschein, J. Mattson, B. Basham, J.D. Sedgwick, et al., IL-23 drives a pathogenic T cell population that induces autoimmune inflammation, J. Exp. Med. 201 (2005) 233–240, https://doi.org/10.1084/jem.20041257.

[29] X. Zhu, S. Li, Q. Zhang, D. Zhu, Y. Xu, P. Zhang, et al., Correlation of increased Th17/Treg cell ratio with endoplasmic reticulum stress in chronic kidney disease, Medicine (Baltimore) 97 (2018) e10748, https://doi.org/10.1097/MD.0000000000010748.

[30] J.M. Pandya, A.C. Lundell, M. Hallstrom, K. Andersson, I. Nordstrom, A. Rudin, Circulating T helper and T regulatory subsets in untreated early rheumatoid arthritis and healthy control subjects, J. Leukoc. Biol. 100 (2016) 823–833, https://doi.org/10.1189/jlb.5A0116-025R.

[31] N.K. Arger, S. Machiraju, I.E. Allen, P.G. Woodruff, L.L. Koth, T-bet expression in peripheral Th17.0 cells is associated with pulmonary function changes in sarcoidosis, Front. Immunol. 11 (2020) 1129, https://doi.org/10.3389/fimmu.2020.01129.

[32] H.J. Park, J.M. Choi, Sex-specific regulation of immune responses by PPARs, Exp. Mol. Med. 49 (2017) e364, https://doi.org/10.1038/emm.2017.102.

[33] M. Morita, M. Mizui, S. Masuyama, G.C. Tsokos, Y. Isaka, Reduction of cell surface T-cell receptor by non-Mitogenic CD3 antibody to mitigate murine lupus, Front. Immunol. 13 (2022) 855812, https://doi.org/10.3389/fimmu.2022.855812.

[34] A. Schnell, D.R. Littman, V.K. Kuchroo, T(H)17 cell heterogeneity and its role in tissue inflammation, Nat. Immunol. 24 (2023) 19–29, https://doi.org/10.1038/s41590-022-01387-9.

[35] K.H.G. Mills, IL-17 and IL-17-producing cells in protection versus pathology, Nat. Rev. Immunol. 23 (2023) 38–54, https://doi.org/10.1038/s41577-022-00746-9.

[36] G. Amarilyo, E.V. Lourenco, F.D. Shi, A. La Cava, IL-17 promotes murine lupus, J. Immunol. 193 (2014) 540–543, https://doi.org/10.4049/jimmunol.1400931.

[37] M. Petric, M. Radic, Is Th17-targeted therapy effective in systemic lupus erythematosus? Curr. Issues Mol. Biol. 45 (2023) 4331–4343, https://doi.org/10.3390/cimb45050275.

[38] L. Sun, J. Fu, Y. Zhou, Metabolism controls the balance of Th17/T-regulatory cells, Front. Immunol. 8 (2017) 1632, https://doi.org/10.3389/fimmu.2017.01632.

[39] B. Raud, D.G. Roy, A.S. Divakaruni, T.N. Tarasenko, R. Franke, E.H. Ma, et al., Etomoxir actions on regulatory and memory T cells are independent of Cpt1a-mediated fatty acid oxidation, Cell Metab. 28 (2018), https://doi.org/10.1016/j.cmet.2018.06.002, 504–515 e507.

[40] A. Wagner, C. Wang, J. Fessler, D. DeTomaso, J. Avila-Pacheco, J. Kaminski, et al., Metabolic modeling of single Th17 cells reveals regulators of autoimmunity, Cell 184 (2021), https://doi.org/10.1016/j.cell.2021.05.045, 4168–4185 e4121.

[41] A. Honda, S. Kamata, M. Akahane, Y. Machida, K. Uchii, Y. Shiiyama, et al., Functional and structural insights into human PPARalpha/delta/gamma subtype selectivity of bezafibrate, fenofibric acid, and pemafibrate, Int. J. Mol. Sci. 23 (2022), https://doi.org/10.3390/ijms23094726.

[42] S. Roedder, N. Kimura, H. Okamura, S.C. Hsieh, Y. Gong, M.M. Sarwal, Significance and suppression of redundant IL17 responses in acute allograft rejection by bioinformatics based drug repositioning of fenofibrate, PLoS One 8 (2013) e56657, https://doi.org/10.1371/journal.pone.0056657.

[43] T. Koltai, Fenofibrate in cancer: mechanisms involved in anticancer activity, F1000Research 4 (2015), https://doi.org/10.12688/f1000research.6153.1.

[44] Y. Yin, S.C. Choi, Z. Xu, D.J. Perry, H. Seay, B.P. Croker, et al., Normalization of CD4+ T cell metabolism reverses lupus, Sci. Transl. Med. 7 (2015) 274ra218, https://doi.org/10.1126/scitranslmed.aaa0835.

[45] Z. Zhang, Z. Zi, E.E. Lee, J. Zhao, D.C. Contreras, A.P. South, et al., Differential glucose requirement in skin homeostasis and injury identifies a therapeutic target for psoriasis, Nat. Med. 24 (2018) 617–627, https://doi.org/10.1038/s41591-018-0003-0.

[46] M. Kono, N. Yoshida, K. Maeda, A. Suarez-Fueyo, V.C. Kyttaris, G.C. Tsokos, Glutaminase 1 inhibition reduces glycolysis and ameliorates lupus-like disease in MRL/lpr mice and experimental autoimmune encephalomyelitis, Arthritis Rheum. 71 (2019) 1869–1878, https://doi.org/10.1002/art.41019.

[47] L. Berod, C. Friedrich, A. Nandan, J. Freitag, S. Hagemann, K. Harmrolfs, et al., De novo fatty acid synthesis controls the fate between regulatory T and T helper 17 cells, Nat. Med. 20 (2014) 1327–1333, https://doi.org/10.1038/nm.3704.

[48] L.E. Raez, K. Papadopoulos, A.D. Ricart, E.G. Chiorean, R.S. Dipaola, M.N. Stein, et al., A phase I dose-escalation trial of 2-deoxy-D-glucose alone or combined with docetaxel in patients with advanced solid tumors, Cancer Chemother. Pharmacol. 71 (2013) 523–530, https://doi.org/10.1007/s00280-012-2045-1.

[49] S.F. Jones, J.R. Infante, Molecular pathways: fatty acid synthase, Clin. Cancer Res. 21 (2015) 5434–5438, https://doi.org/10.1158/1078-0432.CCR-15-0126.

[50] R. Loomba, R. Mohseni, K.J. Lucas, J.A. Gutierrez, R.G. Perry, J.F. Trotter, et al., TVB-2640 (FASN inhibitor) for the treatment of nonalcoholic steatohepatitis: FASCINATE-1, a randomized, placebo-controlled phase 2a trial, Gastroenterology 161 (2021) 1475–1486, https://doi.org/10.1053/j.gastro.2021.07.025.

[51] C. Cortvrindt, R. Speeckaert, A. Moerman, J.R. Delanghe, M.M. Speeckaert, The role of interleukin-17A in the pathogenesis of kidney diseases, Pathology 49 (2017) 247–258, https://doi.org/10.1016/j.pathol.2017.01.003.
[52] M. Durfinova, L. Prochazkova, D. Petrlenicova, Z. Bystricka, K. Oresanska, L. Kuracka, et al., Cholesterol level correlate with disability score in patients with relapsing-remitting form of multiple sclerosis, Neurosci. Lett. 687 (2018) 304–307, https://doi.org/10.1016/j.neulet.2018.10.030.
[53] I. Pineda-Torra, S. Siddique, K.E. Waddington, R. Farrell, E.C. Jury, Disrupted lipid metabolism in multiple sclerosis: a role for liver X receptors? Front. Endocrinol. (Lausanne). 12 (2021) 639757 https://doi.org/10.3389/fendo.2021.639757.
[54] Y. Hao, Y.J. Zhu, S. Zou, P. Zhou, Y.W. Hu, Q.X. Zhao, et al., Metabolic syndrome and psoriasis: mechanisms and future directions, Front. Immunol. 12 (2021) 711060, https://doi.org/10.3389/fimmu.2021.711060.
[55] W. Sondermann, D.A. Djeudeu Deudjui, A. Korber, U. Slomiany, T.J. Brinker, R. Erbel, et al., Psoriasis, cardiovascular risk factors and metabolic disorders: sex-specific findings of a population-based study, J. Eur. Acad. Dermatol. Venereol. 34 (2020) 779–786, https://doi.org/10.1111/jdv.16029.